NANO LETTERS

LETTER

pubs.acs.org/NanoLett

Hybrid Si Microwire and Planar Solar Cells: Passivation and Characterization

Dong Rip Kim, Chi Hwan Lee, Pratap Mahesh Rao, In Sun Cho, and Xiaolin Zheng*

Department of Mechanical Engineering, Stanford University, Stanford, California 94305, United States

Supporting Information

ABSTRACT:

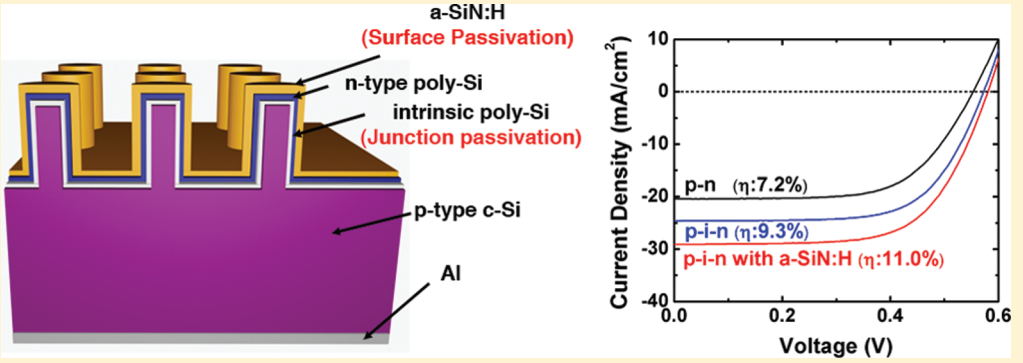

We report an efficient hybrid Si microwire (radial junction) and planar solar cell with a maximum efficiency of 11.0% under AM 1.5G ill;umination. The maximum efficiency of the hybrid cell is improved from 7.2% to 11.0% by passivating the top surface and p−n junction with thin a-SiN:H and intrinsic poly-Si films, respectively, and is higher than that of planar cells of the identical layers due to increased light absorption and improved charge-carrier collections in both wires and planar components.

KEYWORDS: Silicon wire, solar cells, surface and junction passivation, antireflection, radial (core−shell) pn junction, light trapping

Radial junction wire array solar cells, due to the decoupling of light absorption and charge-carrier collection directions, and enhanced light trapping, offer the great opportunity to use lower grade material to produce efficient solar cells.[1−4] Radial junction wire array solar cells have experienced significant development in recent years, and studies have reported efficiencies for single p−i−n Si core/shell nanowires (NWs) of 3.4%,[5] vertically aligned SiNW arrays of 5.3% with junctions formed by a dopant diffusion process,[6] hydrogenated amorphous silicon (a-Si:H) nanodomes of 5.9%,[7] CdS/CdTe core/shell nanopillar arrays of 6.0%,[8] vertical Si microwires (MWs) arrays covered by an amorphous silicon nitride (a-SiN:H) layer, embedded in polymer with Al_2O_3 scatterers of 7.9%,[9] and ultrahigh density SiNW arrays of 10.8% that was fabricated by parallel electron lithography to improve the light absorption percentage to 99%.[10] Nevertheless, radial junction wire array solar cells still face critical challenges such as large surface and interface recombination losses. It is well recognized that the inherent large surface area of the radial junction wire solar cells can lead to large surface and junction recombination of photogenerated charge carriers, which is one of the primary reasons responsible for the gap between reported experimental efficiencies and the estimated 17% theoretical efficiency.[11,12]

Here, we investigated two passivation strategies for the radial junction wire array solar cells. One is to use a thin a-SiN:H layer to passivate the top surface, which is commonly used for bulk Si solar cells[13] and has been demonstrated as an effective passivation/antireflection layer for a horizontal single SiMW photovoltaic device.[14] The other is to use a very thin intrinsic Si layer to passivate the p−n junction, which has been shown to be very effective in the high efficiency a-Si/c-Si heterojunction with intrinsic thin-layer structure (HIT).[15−17] Specifically, the radial junction is consisted of a p-type single-crystalline SiMW core (p-core SiMW) covered by intrinsic and n-type polycrystalline Si (poly-Si) thin layers and an outermost layer of a-SiN:H (Figure 1a). The radial junction is fabricated from a bulk Si wafer to form a hybrid Si MW-planar solar cell to simplify the fabrication process so that we can focus on the passivation methods. The hybrid Si MW-planar solar cell exhibits a maximum of 11.0% solar power conversion efficiency (a mean efficiency of 10.6 ± 0.3%) under a simulated Air Mass 1.5 Global (AM 1.5G) illumination, higher than that of the planar solar cells with the identical layers (a mean efficiency of 8.3 ± 0.5%). The high efficiency of this hybrid structure is a consequence of the following factors. First, the intrinsic and the n-type poly-Si layers simultaneously form and passivate the p−n junction.[17] Second, the a-SiN:H layer both

Received: March 23, 2011
Revised: May 3, 2011
Published: May 24, 2011

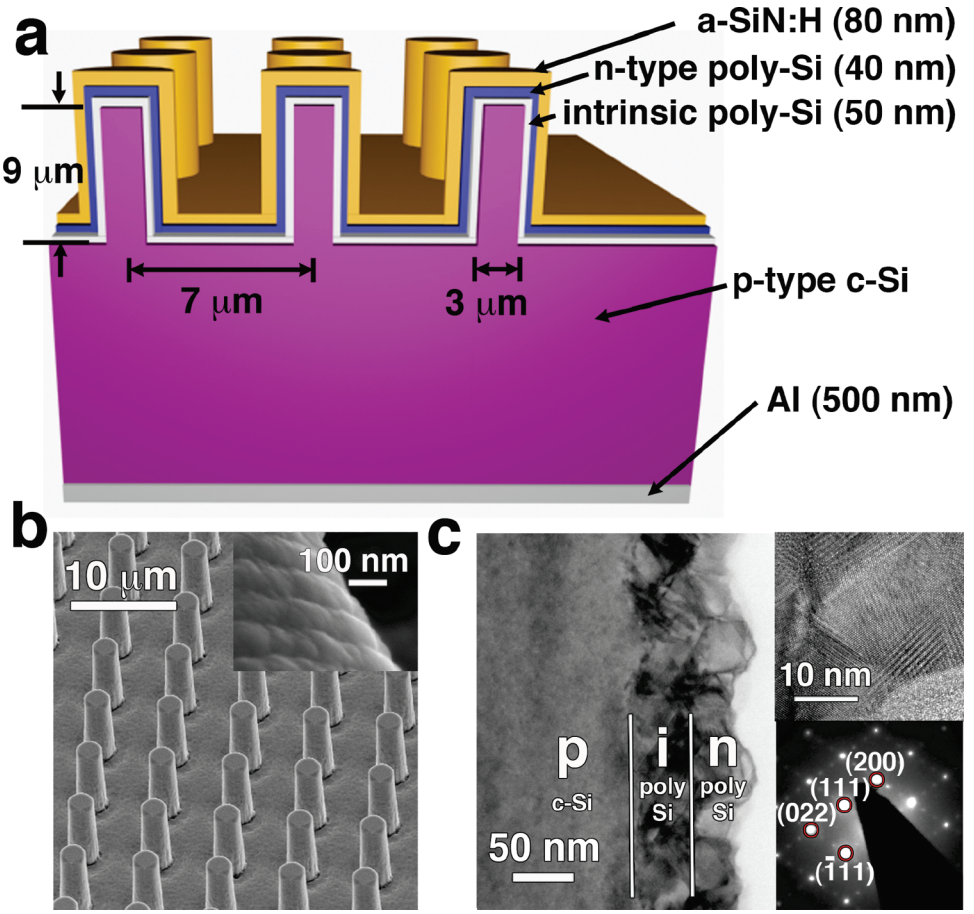

Figure 1. Hybrid Si MW-planar solar cells. (a) Schematic of the hybrid Si MW-planar solar cells (not to scale) which are composed of vertically aligned p-type single-crystalline SiMW (c- SiMW) arrays (diameter, 3 μm; spacing, 7 μm; height, 9 μm) covered with 50 nm thick intrinsic and 40 nm thick n-type polycrystalline-Si (poly-Si) layers, and an outermost 80 nm thick a-SiN:H layer. A 500 nm thick Al layer is used for bottom contacts. (b) SEM images of the hybrid Si MW-planar solar cells. Inset: The coating of the poly-Si layers and the a-SiN:H layer is uniform. (c) TEM images of the sidewalls of the coated SiMWs. Inset (top): Abrupt atomic interfaces within the poly-Si layers with coherent twin boundaries. Inset (bottom): Twin spots of the SAED pattern support the existence of twin boundaries.

passivates the top surface and serves as an antireflection layer.[13] Third, the radial p−n junction structure provides an efficient platform for charge-carrier collection.[3] Finally, the vertically aligned SiMW array traps light for the planar substrate such that more light is absorbed by the top layer where charge carriers can be effectively collected due to shorter diffusion length.

The p-core SiMWs were formed on a 500 μm thick Czochralski (CZ) grade Si(100) wafer (0.1−0.9 Ω·cm) by deep reactive ion etching. The diameter, spacing, and length of the SiMWs are 3 (±0.3) μm, 7 (±0.2) μm, and 9 (±1) μm, respectively. A 50 nm thick intrinsic shell and a 40 nm thick n-type poly-Si shell were deposited on the surface of the p-core SiMWs by using chemical vapor deposition (CVD). We used CVD to form the p−n junction for the easiness in controlling the intrinsic layer thickness and the incorporation of low-quality poly-Si to the device, since the radial junction is most beneficial to low quality material. Nevertheless, both passivation methods should apply to p−n junction formed by other methods such as dopant diffusion and ion implantation. Interestingly, our solar cell with only the i-layer passivation (without including the top a-SiN:H layer) has much higher efficiency (up to 9.3%) than those of similar wire array solar cells fabricated on thick active planar Si (5.7%[18] and 7.2%[19]) where the junction is formed by dopant diffusion. The n-type poly-Si layer has a low resistivity of 0.001−0.002 Ω·cm, which serves as the top contact as well. It should be noted that the current resistivity of the n-type poly-Si layer can limit the device photovoltaic performance and can be further reduced by optimizing its thickness and doping ratio, or by depositing conductive layers on top of it. A 80 nm thick a-SiN:H layer was deposited with plasma-enhanced chemical vapor deposition (PECVD). A 500 nm thick Al layer was metalized as the bottom contact by using electron beam evaporator. The detailed fabrication procedures are described in the Supporting Information and Figure S1. The scanning electron microscopy (SEM) image in Figure 1b shows a typical hybrid Si MW-planar solar cell with evenly spaced and vertically aligned SiMWs. The coating of the poly-Si layers and the a-SiN:H layer is uniform and conformal, as shown in the inset of Figure 1b. A close inspection of the poly-Si layers by cross-section transmission electron microscopy (TEM) (Figure 1c and Supporting Information Figure S2) shows abrupt atomic interfaces within the poly-Si layers (grain sizes 30−100 nm) with coherent twin boundaries. Selected area electron diffraction (SAED) (Figure 1c, bottom inset) clearly supports the existence of the twin boundaries, and a vast majority of the twin boundaries are coherent and lie on the {111} planes (Figure S2, Supporting Information).[20,21] The coherent twin boundaries within the

Table 1. Average Photovoltaic Properties of Hybrid Si MW-Planar Cells and Planar Si Solar Cells

	structure	V_{oc} (V)	J_{sc} (mA/cm^2)	FF	η (%)
hybrid solar cell	p−n	0.541 ± 0.012	20.3 ± 0.4	0.617 ± 0.013	6.8 ± 0.2
	p−i−n	0.560 ± 0.011	24.4 ± 0.7	0.653 ± 0.023	8.9 ± 0.2
	p−i−n (a-SiN:H)	0.558 ± 0.016	30.6 ± 0.9	0.625 ± 0.038	10.6 ± 0.3
planar solar cell	p−n	0.563 ± 0.006	19.3 ± 1.1	0.589 ± 0.037	6.4 ± 0.7
	p−i−n	0.563 ± 0.010	20.2 ± 0.4	0.597 ± 0.041	6.8 ± 0.4
	p−i−n (a-SiN:H)	0.557 ± 0.015	26.3 ± 0.8	0.571 ± 0.036	8.3 ± 0.5

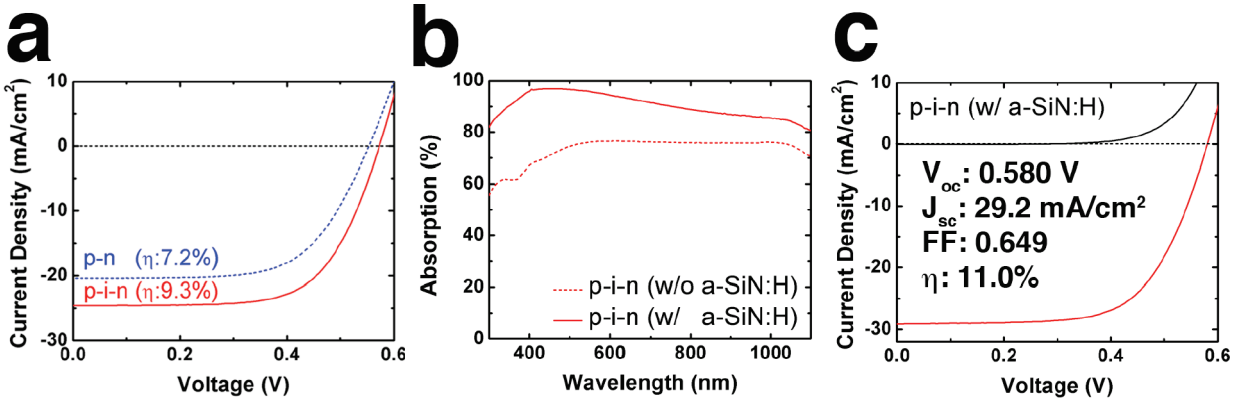

Figure 2. The photovoltaic properties of the hybrid Si MW-planar solar cells. (a) Effect of the intrinsic layer on the photovoltaic properties of the hybrid Si MW-planar solar cells. The percentages of the 7.2% (p−n) and 9.3% (p−i−n) cell's planar section area are 76% and 64%, respectively. (b) The light absorption of the hybrid Si MW-planar solar cells as functions of the wavelength with (solid line) and without the a-SiN:H layer (dashed line). (c) The light J−V curve of the best hybrid Si MW-planar solar cell. The percentage of the best cell (11.0%, p−i−n with a-SiN:H)'s planar section area is 64%. We confirmed, through multiple experiments, that the improvements of photovoltaic properties of our solar cells are indeed from passivation strategies, not from the variations in the percentage of the cell's planar area.

poly-Si layers are electrically inactive and have reduced interfacial recombination compared to randomly oriented grain boundaries in poly-Si.[22] In addition, poly-Si is more stable than hydrogenated a-Si:H under prolonged illumination because of its higher degree of crystallinity and smaller hydrogen content.[23] These two characteristics of the poly-Si are both beneficial to solar cells.

First, the effect of the intrinsic poly-Si layer on the performance of the hybrid Si MW-planar solar cell was investigated since the intrinsic layer has been shown to effectively reduce the dark current density (J_0) in both the vertical HIT[17] and the p−i−n core/shell SiNW structures.[5] The top a-SiN:H layer was not included here in order to identify the role of the intrinsic layer. Linear fitting of the current density−voltage ($\ln(J)-V$) curves of the radial p−n and p−i−n hybrid Si MW-planar solar cells yields diode ideality factors (n) of 2.45 ± 0.11 and 1.89 ± 0.14, and dark current densities (J_0) of 500−1700 and 32−155 nA/cm^2, respectively. The improved n and more than 1 order of magnitude reduced J_0 clearly demonstrate the reduction in junction recombination by the passivating effect of the intrinsic layer.[5] The effectiveness of the intrinsic layer is further illustrated by comparing the photovoltaic properties (Table 1) and the light $J-V$ curves (Figure 2a), which shows that the intrinsic poly-Si passivation layer increases the mean open circuit voltage (V_{oc}), the mean short circuit current density (J_{sc}), and the mean efficiency (η) by 4%, 20%, and 31%, respectively.

Next, we examine the effect of the outermost a-SiN:H layer on the light absorption and photovoltaic properties of the hybrid Si MW-planar solar cells. The inclusion of the outermost 80 nm thick a-SiN:H layer increases the integrated light absorption percentage of the hybrid Si MW-planar solar cells from 74% to 92% (Figure 2b), which is integrated light absorption over the wavelength range from 280 to 1100 nm normalized by that of the AM 1.5G spectrum. The increase of the overall light absorption is due to the fact that the a-SiN:H layer (refractive index 1.95) serves as an effective antireflective coating[24] between air and Si. It should be noted that the light absorption peak shift toward shorter wavelengths for the hybrid Si MW-planar solar cells (Figures 2b and 3b) compared to the planar cells with identical top layers (i.e., the light absorption peak around wavelengths of 600 nm with 80 nm thick a-SiN:H) is attributed to the reduced conformity of deposition of the a-SiN:H layer onto the high-aspect ratio SiMWs by PECVD,[12] and therefore, the decreased average thickness of the a-SiN:H layer on the sidewalls of the SiMWs deviates from the optimal 80 nm thickness for antireflection between air and Si.

Furthermore, the inclusion of the outermost a-SiN:H layer greatly enhances the photovoltaic properties (Figure 2c and Table 1) of the hybrid Si MW-planar solar cell. The outermost a-SiN:H layer increases the mean short circuit current density (J_{sc}) and the mean efficiency (η) by 25% and 19%, respectively. The major part of the improvement comes from the antireflection effect and the rest comes from the surface passivation effect[13,14] of the PECVD-deposited a-SiN:H that has the reduced density of surface states and positive interface charges.[13] Consequently, the hybrid Si MW-planar solar cells with both the intrinsic and a-SiN:H layers exhibit a mean efficiency of

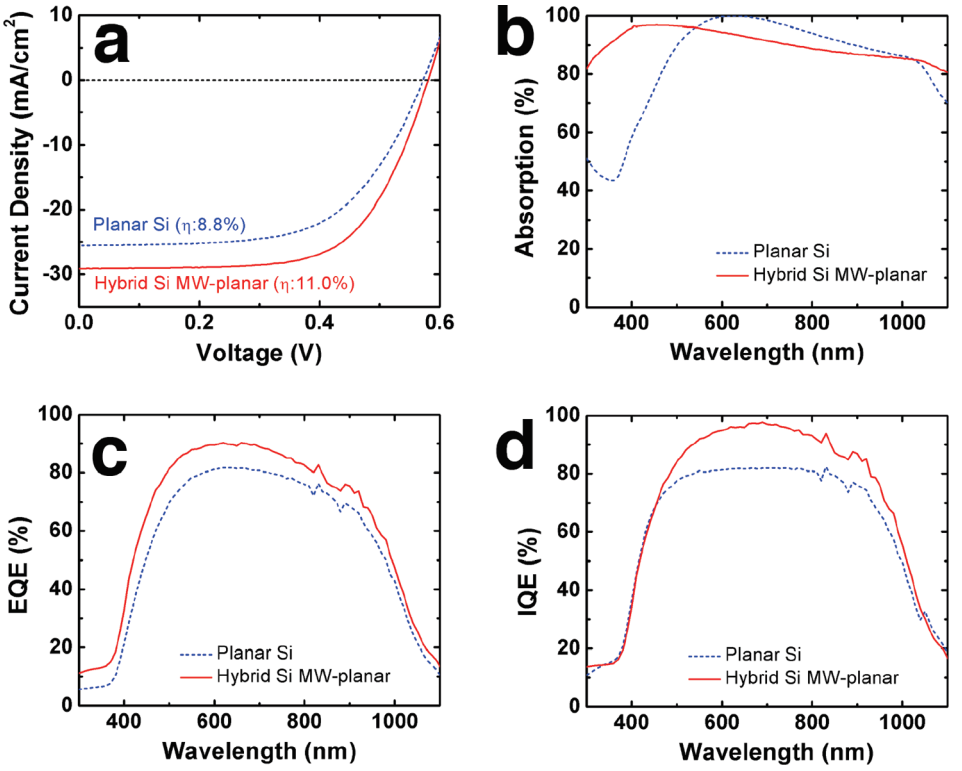

Figure 3. Comparisons of the hybrid Si MW-planar solar cell to the planar Si solar cell. (a) Light $J-V$ curves of the hybrid Si MW-planar solar cell (η, 11.0%; V_{oc}, 0.580 V; J_{sc}, 29.2 mA/cm^2; and FF, 0.649) and the planar Si solar cell (η, 8.8%; V_{oc}, 0.575 V; J_{sc}, 25.5 mA/cm^2; and FF, 0.602). (b) The light absorption percentages as functions of the wavelength. The integrated light absorption is about 92% for the hybrid Si MW-planar cell and 88% for the planar Si cell. (c, d) External (c) and internal quantum efficiencies (d) as functions of the wavelength. The hybrid Si MW-planar solar cell exhibits higher quantum efficiencies than the planar Si cell in the visible light and infrared regimes.

$10.6 \pm 0.3\%$ (V_{oc} of 0.558 ± 0.016 V, J_{sc} of 30.6 ± 0.9 mA/cm^2, and FF of 0.625 ± 0.038) (Table 1), and a maximum efficiency of 11.0% (V_{oc} of 0.580 V, J_{sc} of 29.2 mA/cm^2, and FF of 0.649) (Figure 2c). In addition, such good performance is consistently observed over many devices (Table S1, Supporting Information). It should be noted that the SiMW arrays in the current hybrid cell are surrounded by planar Si margins for probe contacting to prevent the probes from breaking the MWs during the $J-V$ measurement (see Figure S3, Supporting Information). The planar section area occupies about 60−76% of the total projected area and is included in the calculation of J_{sc} and η. Since the planar Si section has lower efficiency than the MW arrays as discussed below (Figure 3), we believe that the efficiency and the light absorption percentage can be improved further by increasing the coverage density of SiMWs and reducing the spacing between SiMWs, as seen in the recently reported ultrahigh density wire arrays.[10]

Finally, we compare, in Figure 3, the performance of the hybrid Si MW-planar solar cell with a planar solar cell which has the identical thicknesses of the intrinsic poly-Si, n-type poly-Si, and a-SiN:H layers, deposited simultaneously under identical experimental conditions. The only difference is that SiMWs are not formed by dry etching on top of the planar cells. First, although the hybrid solar cell has larger top surface and p−n junction areas, its V_{oc} and FF are comparable to the planar case (Figure 3a), suggesting that the top surface and the p−n junction interface are well passivated by the a-SiN:H layer and the intrinsic poly-Si layer, respectively. Second, the hybrid solar cell has about 1.2 times higher J_{sc} than that of the planar cell (Figure 3a), although the amount of integrated light absorption percentage is similar in both cases, i.e., about 92% for the hybrid cell and 88% for the planar Si cell (Figure 3b and Figure S4 in the Supporting Information). Therefore, the 20% higher J_{sc} in the hybrid structure (Figure 3a) cannot be explained solely on the basis of enhanced light absorption. As shown in panels c and d of Figure 3, the hybrid cell has higher external and internal quantum efficiencies (IQEs) than the planar Si over a broad range of wavelengths, particularly in the visible light and infrared regimes. Especially, the higher IQEs of the hybrid cell (Figure 3d), which excludes the light absorption difference, strongly indicate that the hybrid cell is more efficient in charge separation and collection. Part of the efficiency enhancement comes from the efficient charge-carrier collection in the radial p−n junction structure of the SiMWs. In addition, the SiMW arrays can bounce and redirect light to the planar Si substrate to increase the charge-carrier generations near the p−i−n junction of the Si substrate, which, in turn, can facilitate the collection of charge carriers due to the reduced diffusion length. The low quantum efficiencies in the short wavelength regime for both the hybrid and the planar cell (Figure 3c,3d) are due to emitter loss in the poly-Si layers, so their thicknesses should be kept as thin as possible.[15,16,25] These comparisons strongly suggest that adding radial junction MWs on top of planar solar cells can greatly improve the photovoltaic properties of the planar cells, especially when using low-quality materials with short minority carrier diffusion length.[26]

In summary, we have experimentally demonstrated that the hybrid Si MW-planar solar cells exhibit higher efficiencies

(a maximum of 11.0% and an average of 10.6 ± 0.3%) than those of planar solar cells of the identical layers. The high efficiency stems from the effective passivation of both the p−n junction and the top surface by the intrinsic poly-Si layer and the a-SiN:H layer, respectively, and the strong antirefection effect of the a-SiN:H layer, together with the structural merits of the radial junction SiMW arrays, which not only have efficient charge-carrier collection in themselves but also improve the carrier collection in the planar substrate. Furthermore, the hybrid solar cells are fabricated by simple one-step photolithography, dry etching, and intermediate temperature deposition processes with the potential of lowering fabrication cost by replacing poly-Si with heterojunction materials such as hydrogenated a-Si:H or nanocrystalline Si:H. We believe that the efficiency of the hybrid solar cells can be further improved by optimizing the geometries of the wire arrays and the thicknesses and deposition conditions of the three thin film layers, by passivating the bottom surface, and by increasing the coverage density of SiMWs. More importantly, our junction and surface passivation strategies should be applicable to all the radial junction wire array solar cells. Finally, the hybrid MW-planar structure can serve as an important intermediate between planar solar cells and pure wire array solar cells, which has higher efficiency than planar comparison solar cells and simpler fabrication steps than pure wire array solar cells.

■ ASSOCIATED CONTENT

Supporting Information. Detailed materials and methods used in this work. This material is available free of charge via the Internet at http://pubs.acs.org.

■ AUTHOR INFORMATION

Corresponding Author
*E-mail: xlzheng@stanford.edu.

■ ACKNOWLEDGMENT

D.R.K. and P.M.R. acknowledge support from the Link Foundation Energy Fellowship. X.L.Z. acknowledges support from the Center on Nanostructuring for Efficient Energy Conversion, an Energy Frontier Research Center funded by the U.S. Department of Energy, Office of Science, Office of Basic Energy Sciences under Award Number DE-SC0001060. The authors also thank Dr. Ann F. Marshall at Stanford University for the helpful discussions on the cross-section TEM sample preparations and TEM images.

■ REFERENCES

(1) Boettcher, S. W.; Spurgeon, J. M.; Putnam, M. C.; Warren, E. L.; Turner-Evans, D. B.; Kelzenberg, M. D.; Maiolo, J. R.; Atwater, H. A.; Lewis, N. S. *Science* **2010**, *327*, 185–187.
(2) Lewis, N. S. *Science* **2007**, *315*, 798–801.
(3) Kayes, B. M.; Atwater, H. A.; Lewis, N. S. *J. Appl. Phys.* **2005**, *97*, 114302–114311.
(4) Peng, K.-Q.; Lee, S.-T. *Adv. Mater.* **2011**, *23*, 198–215.
(5) Tian, B. Z.; Zheng, X. L.; Kempa, T. J.; Fang, Y.; Yu, N.; Yu, G.; Huang, J.; Lieber, C. M. *Nature* **2007**, *449*, 885–888.
(6) Garnett, E.; Yang, P. D. *Nano Lett.* **2010**, *10*, 1082–1087.
(7) Zhu, J.; Hsu, C. M.; Yu, Z. F.; Fan, S. H.; Cui, Y. *Nano Lett.* **2010**, *10*, 1979–1984.
(8) Fan, Z.; Razavi, H.; Do, J.; Moriwaki, A.; Ergen, O.; Chueh, Y.-L.; Leu, P. W.; Ho, J. C.; Takahashi, T.; Reichertz, L. A.; Neale, S.; Yu, K.; Wu, M.; Ager, J. W.; Javey, A. *Nat. Mater.* **2009**, *8*, 648–653.
(9) Putnam, M. C.; Boettcher, S. W.; Kelzenberg, M. D.; Turner-Evans, D. B.; Spurgeon, J. M.; Warren, E. L.; Briggs, R. M.; Lewis, N. S.; Atwater, H. A. *Energy Environ. Sci.* **2010**, *3*, 1037–1041.
(10) Lu, Y.; Lal, A. *Nano Lett.* **2010**, *10*, 4651–4656.
(11) Kelzenberg, M. D.; Turner-Evans, D. B.; Kayes, B. M.; Filler, M. A.; Putnam, M. C.; Lewis, N. S.; Atwater, H. A. *Proc. IEEE Photovoltaic Spec. Conf., 33rd* **2008**, 1−6.
(12) Kelzenberg, M. D.; Boettcher, S. W.; Petykiewicz, J. A.; Turner-Evans, D. B.; Putnam, M. C.; Warren, E. L.; Spurgeon, J. M.; Briggs, R. M.; Lewis, N. S.; Atwater, H. A. *Nat. Mater.* **2010**, *9*, 239–244.
(13) Aberle, A. G. *Prog. Photovoltaics* **2000**, *8*, 473–487.
(14) Kelzenberg, M. D.; Turner-Evans, D. B.; Putnam, M. C.; Boettcher, S. W.; Briggs, R. M.; Baek, J. Y.; Lewis, N. S.; Atwater, H. A. *Energy Environ. Sci.* **2011**, *4*, 866–871.
(15) Fujiwara, H.; Kondo, M. *J. Appl. Phys.* **2007**, *101*, 054516.
(16) Tanaka, M.; Taguchi, M.; Matsuyama, T.; Sawada, T.; Tsuda, S.; Nakano, S.; Hanafusa, H.; Kuwano, Y. *Jpn. J. Appl. Phys.* **1992**, *31*, 3518–3522.
(17) Sawada, T.; Terada, N.; Tsuge, S.; Baba, T.; Takahama, T.; Wakisaka, K.; Tsuda, S.; Nakano, S. *Proc. IEEE World Conf. Photovoltaic Energy Convers., 1st* **1994**, 1219−1226.
(18) Kayes, B. M.; Filler, M. A.; Henry, M. D.; Maiolo, J. R., III; Kelzenberg, M. D.; Putnam, M. C.; Spurgeon, J. M.; Plass, K. E.; Scherer, A.; Lewis, N. S.; Atwater, H. A. *Proc. IEEE Photovoltaic Spec. Conf., 33rd* **2008**, 1−5.
(19) Jung, J.-Y.; Guo, Z.; Jee, S.-W.; Um, H.-D.; Park, K.-T.; Hyun, M. S.; Yang, J. M.; Lee, J.-H. *Nanotechnology* **2010**, *21*, 445303.
(20) Migliorato, P.; Meakin, D. B. *Appl. Surf. Sci.* **1987**, *30*, 353–371.
(21) Bender, H.; Deveirman, A.; Vanlanduyt, J.; Amelinckx, S. *Appl. Phys. A: Mater. Sci. Process.* **1986**, *39*, 83–90.
(22) Farrenbruch, A. L.; Bube, R. H. *Fundamentals of solar cells: photovoltaic solar energy conversion*; Academic Press: New York, 1983.
(23) Funde, A. M.; Bakr, N. A.; Kamble, D. K.; Hawaldar, R. R.; Amalnerkar, D. P.; Jadkar, S. R. *Sol. Energy Mater. Sol. Cells* **2008**, *92*, 1217–1223.
(24) Green, M. A. *Solar cells: operating principles, technology, and systems applications*; Prentice Hall: Englewood Cliffs, NJ, 1982.
(25) Jensen, N.; Hausner, R. M.; Bergmann, R. B.; Werner, J. H.; Rau, U. *Prog. Photovoltaics* **2002**, *10*, 1–13.
(26) Yoon, H. P.; Yuwen, Y. A.; Kendrick, C. E.; Barber, G. D.; Podraza, N. J.; Redwing, J. M.; Mallouk, T. E.; Wronski, C. R.; Mayer, T. S. *Appl. Phys. Lett.* **2010**, *96*, 213503.

■ NOTE ADDED AFTER ASAP PUBLICATION

The TOC and abstract artwork was incorrect in the version of this paper published May 24, 2011. The correct version published May 27, 2011.